Nonlinear Processes in Geophysics (1999) 6: 11–26

Nonlinear Processes in Geophysics

Internal gravity waves: Analysis using the periodic, inverse scattering transform

W. B. Zimmerman[1] and G. W. Haarlemmer[2]

[1]Department of Chemical and Process Engineering, University of Sheffield, Newcastle Street, Sheffield S1 3RD, England
[2]Department of Chemical Engineering, UMIST, P.O. Box 88, Manchester M60 1QD, England

Received: 11 January 1999 – Accepted: 19 February 1999

Abstract. The discrete periodic inverse scattering transform (DPIST) has been shown to provide the salient features of nonlinear Fourier analysis for surface shallow water waves whose dynamics are governed by the Korteweg-de Vries (KdV) equation – (1) linear superposition of components with power spectra that are invariants of the motion of nonlinear dispersive waves and (2) nonlinear filtering. As it is well known that internal gravity waves also approximately satisfy the KdV equation in shallow stratified layers, this paper investigates the degree to which DPIST provides a useful nonlinear spectral analysis of internal waves by application to simulations and wave tank experiments of internal wave propagation from localized dense disturbances. It is found that DPIST analysis is sensitive to the quantity $\lambda = \frac{r}{6s}\frac{\epsilon}{\mu^2}$, where the first factor depends parametrically on the Richardson number and the background shear and density profiles and the second factor is the Ursell number–the ratio of the dimensionless wave amplitude to the dimensionless squared wavenumber. Each separate wave component of the decomposition of the initial disturbance can have a different λ value, and thus there is usually just one component which is an invariant of the motion found by DPIST analysis. However, as the physical applications, e.g. accidental toxic gas releases, are usually concerned with the propagation of the longest wavenumber disturbance, this is still useful information. In cases where only long, monochromatic solitary waves are triggered or selected by the waveguide, the entire DPIST spectral analysis is useful.

1 Motivation

An attractive idea for the data analysis of spatiotemporal waves in a one dimensional wave-guide has been championed over many years by A.R. Osborne and co-workers: Osborne and Petti (1994), Osborne and Segre (1993), Osborne and Petti (1993), Osborne (1991), Osborne et al. (1991), Osborne and Segre (1990), Osborne and Bergamasco (1986), Osborne and Bergamasco (1985). The workhorse technique of data analysis of wave propagation is the discrete, fast Fourier transform. Perhaps the single most important feature of the Fourier transform for application to wave motion is the linear superposition principle for components that are invariant during the propagation of linear, dispersive waves. The crux of the new data analysis technique is the analogous treatment of nonlinear dispersive waves. The discrete, periodic inverse scattering transform has a linear superposition principle for components that are invariant during the propagation of nonlinear, dispersive waves governed by integrable dynamics.

The focus of the work by Osborne and co-workers has been the dynamics of shallow water surface waves, which approximately satisfy the Korkweg-de Vries (KdV) equation [Korteweg and de Vries (1894)]. The KdV equation is well known to be integrable (see e.g. Lamb (1980)) and thus tractable for the solution of initial value problems by the inverse scattering transform. The focus of Osborne and Bergamasco [Osborne and Bergamasco (1986), Osborne and Bergamasco (1985)] was to implement numerically the discrete, periodic inverse scattering transform. (DPIST) as a data analysis technique completely analogous to Fourier analysis but in a nonlinear sense for weakly nonlinear shallow water surface waves. Once the data analysis tool was vetted, application to ocean surface waves [Osborne et al. (1991)] and laboratory-generated shallow water waves [Osborne and Petti (1994)] demonstrated the robustness of the technique. As these situations only approximately satisfy the KdV equations, and then only perhaps in narrow regimes of validity, the success of the technique lends credibility to the speculation that it may be more generally applicable to other applications where the KdV equation is a valid approximation: internal waves [Ben-

Correspondence to: Dr. Zimmerman

ney (1966), Benjamin (1966)], Rossby waves [Benney (1966), Long (1964), Maxworthy and Redekopp (1976)], and bores [Peregrine (1966)].

In this paper, the challenge of applying DPIST for data analysis of internal gravity waves is taken up. Simulations and wave tank experiments of internal gravity wave propagation from localized, dense releases are performed to generate datasets which, based on the theories of [Benney (1966)] and [Benjamin (1966)] and subsequent developments [Maslowe and Redekopp (1980), Gear and Grimshaw (1983), Weidman and Velarde (1992), Koop and Butler (1981)], would be expected to develop into nonlinear dispersive waves governed approximately by the KdV equation. The simulations are of a two-dimensional atmospheric inversion with initial releases of cold disturbances that later develop into solitary waves. The wave tank experiments, also modelling this situation, are undertaken to produce less idealized data sets of internal wave propagation. Some modelling choices for the parameters of the DPIST method are made which make the analysis plausible. Discussion of the applicability of DPIST to internal wave data follows.

In the next subsection, the paradigm of the inverse scattering transform is reviewed and the organization of the paper explained.

1.1 The Paradigm of the Inverse Scattering Transform

A transform frequently encountered in the theoretical treatment of nonlinear dispersive waves is the Inverse Scattering Transform (IST). This is a spectral analysis technique for wave motion governed by specific nonlinear evolution equations. In this paper, the focus is on the KdV equation.

Osborne and Bergamasco (1985) showed that the scattering transform reduces to a Fourier series in the vanishing amplitude limit. The shape functions used in scattering, however, take a different form than the Fourier series. The analogues of sines and cosines for the linear Fourier theory are the hyperelliptic functions (μ_j) for the scattering transform. In absence of nonlinear interactions these μ_j's are cnoidal waves and in the simple one soliton case they can be a sech^2 (Osborne and Bergamasco (1986)). When more than one mode is present there will be a nonlinear interaction between the modes. The oscillation modes are no longer pure cnoidal waves since the interaction term must be accommodated.

DPIST is not limited to situations that are approximated by KdV dynamics. For instance, it has been used to analyze disturbances propagating in the Toda lattice. The Toda lattice, or Toda chain in one dimension, models vibrations in solids. Fermi et al. (1955) performed seminal numerical simulations in which they introduced disturbances in the Toda chain. IST for solitary waves propagating through the Toda chain is now a much studied topic [Flashka (1974), Flashka and McLaughlin (1976) and Ferguson et al. (1982)].

The essence of DPIST is to compute discrete approximations to the spectra of the Schrödinger equation, where the potential $u(x)$ is given by the initial profile of the wave: $u(x) = \lambda\eta(x, t = 0)$, where λ is a parameter expressing the degree of nonlinearity of the waveform, and $\eta(x, t)$ is the waveform. $\eta(x, t = 0)$ is termed the signal. The information produced by DPIST analysis consists of a main spectrum, an auxiliary spectrum (with oscillation modes) and the amplitudes of the oscillation modes. A linear affine combination of the oscillation modes requiring all of the information obtained by DPIST reconstructs the original signal. When the wave motion is governed by the KdV equation, the amplitudes of the oscillation modes are invariants of the motion. Thus the waveform at all subsequent times may be constructed by information extracted by DPIST from the initial signal only.

In section 2 the scattering algorithm used in this study is explained. Further, the inverse problem and time evolution of waves are explored. Examples and tests of the scattering transform are given in section 3. The application of the scattering transform to the wave data of the simulations in this paper is discussed in section 4. Some experiments are analysed in section 5. Concluding remarks are made in section 6.

2 Application of the scattering transform to wave in fluids

2.1 Korteweg de Vries equation and Scalings

The Korteweg and de Vries equation for weakly nonlinear, shallow water surface waves is:

$$\eta^*_{t^*} + c_0\eta^*_{x^*} + \alpha^*\eta^*\eta^*_{x^*} + \beta^*\eta^*_{x^*x^*x^*} = 0 \tag{1}$$

The asterisk refers to dimensional variables. In this equation the various constants are specific for the medium in which the wave propagates. In the case of shallow water surface waves: $\eta^*(x, t)$ is the wave amplitude as a function of space and time, $\alpha^* = 3c_0/2h$, $\beta^* = c_0h^2/6$, c_0 is the linear, long wave phase speed $c_0 = \sqrt{gh}$ and h the height of the water surface. It is convenient to restate (1) in dimensionless variables with scalings

$$\eta = \frac{\eta^*}{A_0}, \qquad t = \frac{t^*}{h/c_0}, \qquad x = \frac{x^*}{L} \tag{2}$$

These scalings are explained below. The KdV equation takes the form:

$$\eta_t + \eta_x + \alpha\eta\eta_x + \beta\eta_{xxx} = 0 \tag{3}$$

with $\alpha = \frac{3}{2}\varepsilon$ and $\beta = \frac{1}{6}\mu^2$. The KdV equation is rewritten in order for it to be solvable by a scattering method. The amplitude η is substituted by (Whitham (1974)).

$$u(x) = -\frac{\alpha}{6\beta}\eta(x, t = 0) = -\lambda\eta(x, t = 0) \tag{4}$$

Here λ is a parameter indicating the degree of nonlinearity of the wave, a modified Ursell number. The KdV equation is rewritten in a more convenient form in a moving coordinate system $x \leftarrow x - t$:

$$u_t - 6uu_x + u_{xxx} = 0 \tag{5}$$

Benney (1966) showed for shear and stable stratification of weakly nonlinear, long waves in a shallow layer:

$$\alpha = \varepsilon \frac{3}{2c} \frac{\int_0^1 \hat{\rho}\,(c-\hat{u})^2\,\phi_z^3 dz}{\int_0^1 \hat{\rho}\,(c-\hat{u})^2\,\phi_z^2 dz} = \varepsilon \frac{r}{c} \tag{6}$$

$$\beta = \mu^2 \frac{1}{2c} \frac{\int_0^1 \hat{\rho}\,(c-\hat{u})^2\,\phi^2 dz}{\int_0^1 \hat{\rho}\,(c-\hat{u})^2\,\phi_z^2 dz} = \mu^2 \frac{s}{c} \tag{7}$$

where $\hat{\rho}(z)$ and $\hat{u}(z)$ are the dimensionless background density and velocity profiles. The vertical scaling is h, the height of the fluid layer, and the horizontal, L the wavelength of the long wave; for velocities γh, where γ is the characteristic shear rate; for time γ^{-1}; for density, ρ_0, the density at the bottom bounding surface, where ε is the ratio of the amplitude of the wave A_0 to the height of the waveguide and μ is the ratio of the same height to the wavelength L.

The eigenfunction $\phi(z)$ and eigenvalue c is found from the linearized equations of motion, which in the inviscid, long wave approximation gives the Taylor-Goldstein boundary value problem [Taylor (1931); Goldstein (1931)]:

$$L\{\phi\} = \left[\hat{\rho}\,(\hat{u}-c)^2\,\phi_z\right]_z + \hat{\rho}\hat{N}Ri\phi = 0 \tag{8}$$

$$\phi|_{z=0} = \phi|_{z=1} = 0 \tag{9}$$

The above boundary value problem also yields the eigenvalue $c = c_n$ for $n = \pm 1, \pm 2, \pm 3, \ldots$ and corresponding modes $\phi_n(z)$. c depends only on the waveguide shear profile $\hat{u} = \hat{\psi}_z$, the stratification $\hat{\rho}$, and the Richardson number $Ri = N^2/\gamma^2$. N is the characteristic Brunt-Väisälä frequency. $\hat{N}(z)$ is the dimensionless Brunt-Väisälä frequency.

Such detail in the Korteweg-de Vries approximation to surface shallow water waves and to internal gravity waves modified by shear is to demonstrate the fundamental differences in the coefficients α and β in the two cases.

- For surface shallow water waves:

$$\lambda = \frac{3}{2}\frac{\varepsilon}{\mu^2}$$

- For internal gravity waves modified by shear:

$$\lambda = \frac{r}{6s}\frac{\varepsilon}{\mu^2}$$

The fundamental parameter for the scattering transform, λ, in both cases depends on the characteristics of the nonlinear dispersive waves that are generated – the nonlinearity ε and the wave-number (through μ^2). In the case of surface waves, it depends only on this. For internal gravity waves modified by shear, it depends on the ratio s/r which is a functional of $\hat{\rho}(z)$ and $\hat{u}(z)$ and parametrically dependent on Ri. Zimmmerman and Velarde (1999) discuss the role of s/r in Couette flow with linear stratification in constraining solitary wave propagation as a function of Ri.

Experimentally, in a shallow water wave tank, the wavemaker can be programmed to produce the desired amplitude and wavenumber and thus λ is fixed. The experiments of Osborne and Petti (1994) were so controlled. In their experiments, care was taken so that λ is placed in the regime of validity of the KdV approximation. In a stratified, sheared wind tunnel, for instance, generating backgrounds with fixed s/r is in principle possible, but controlling the waves generated is more problematic. In stratified wave tanks, introducing shear is difficult, as is generating large amplitude solitary waves with tightly controlled characteristics. In the simulations of internal wave propagation and in the wave tank experiments performed here, no attempt is made to set the Ursell number $\mathrm{Ur} = \frac{\varepsilon}{\mu^2}$ for monochromatic waves, but rather initial localized disturbances are permitted to evolve in known background conditions. The resulting waves from the decomposition of the initial disturbance may have λ substantially different from the initial disturbance. Thus, for DPIST to provide a practical spectral analysis of the internal wave data from the simulations and expermenents performed here, it must be a robust technique in the face of uncertainty in λ.

2.2 Scattering equations

The Schrödinger equation is (Lamb (1980)):

$$\psi_{xx} + [E - u(x)]\psi = 0 \tag{10}$$

The KdV equation (5) was linked to the Schrödinger equation by Gardner et al. (1967). They solved the Schrödinger equation with a potential well $u(x)$ (signal) constrained to satisfy the KdV equation and showed that the oscillation modes found are a solution to the KdV equation. This method allows the prediction of the number of solitons that emerge from an initial condition $u(x)$. When the time evolution of the signal is governed by the KdV equation, the amplitude of the various components remains constant in time. This is provided that the correct coefficients (and thus λ) of the KdV equation are known.

E is loosely termed the eigenvalue, which according to the condition imposed on the basis functions of (10), will be deemed to be in the main spectrum or the auxillary spectrum. Additionally, the auxiliary spectrum translated over the entire interval $[0, L]$ gives the μ_j-function oscillation modes. The amplitudes of these modes are readily computed from the spectral energies. To compute the nonlinear power spectrum of a signal $\eta(x,t)$, (10) is integrated to find the eigenvalues and basis func-

tions. A simple approach can be taken in solving (10) using a Runge-Kutta shooting method to find the eigenvalues E. However, numerical integration of the hyperelliptic functions μ_j is difficult as they are strongly coupled (Osborne and Segre (1990)) so the inverse problem is ill-conditioned. To overcome this problem and to speed up the computation, a new algorithm was developed by Osborne and co-workers. The DPIST algorithm used here to compute the scattering transform is taken from Osborne and Segre (1993) and summarized below for completeness.

2.3 Numerical algorithm

It is assumed that the signal and its subsequent evolution are periodic, with period L, so that $\eta(x,t) = \eta(x+L,t)$. x_0 is taken as an arbitrary base point on the interval $[0,L]$. A basis of normalised independent functions is introduced:

$$\mathbf{\Phi}(x;x_0,E) = \begin{pmatrix} \phi & \phi_x \\ \phi^* & \phi_x^* \end{pmatrix} = \begin{pmatrix} 1 & ik \\ 1 & -ik \end{pmatrix}_{x=x_0=0} \quad (11)$$

The initial condition above ensures independence of the four basis functions. It is possible to express the basis functions at an arbitrary point $x+L$ with x on the interval $[0,L]$ in terms of the basis functions at point x. Basis functions at spatial point $x+L$ can be expressed in terms of the basis functions at x:

$$\mathbf{\Phi}(x+L;x_0,E) = \mathbf{S}(x_0,E)\mathbf{\Phi}(x;x_0,E) \quad (12)$$

The matrix $\mathbf{S}(x_0,E)$ is the monodromy matrix. See also Flashka and McLaughlin (1976) for a more detailed outline of the theory. This matrix constrains E to define the main and the auxiliary spectra of the scattering transform. The main spectrum determines the set of eigenvalues E_i (with $1 \le i \le 2N+1$ with N the number of spectral components). It determines the amplitudes of the oscillation modes μ_j. For computational reasons the complex matrix is avoided by rewriting the initial values of the basis, normalised at x_0:

$$\begin{aligned} \mathbf{\Phi}(x_0,x_0,E) &= \begin{pmatrix} \cos x_0 & -\sin x_0 \\ \sin x_0 & \cos x_0 \end{pmatrix} \\ &= \begin{pmatrix} 1 & -0 \\ 0 & 1 \end{pmatrix}\Big|_{x_0=0} \end{aligned}$$

The new basis permits calculations with only real numbers, a significant feature for efficient coding and computation speed. On this new basis the Floquet discriminant can be found in the trace of the new monodromy matrix $\mathbf{\Theta}$ that describes the integration from point x on $[0,L]$ to $x+L$. The main spectrum is found where the trace of this matrix equals ± 1.

Main spectrum ($E = E_i$):
$Tr\left[\mathbf{\Theta}(E)\right] = \frac{1}{2}\left(\Theta_{11}(E) + \Theta_{22}(E)\right) = \pm 1$
Auxiliary spectrum ($E = \mu_j\,(x=0,t=0)$):
$\Theta_{21} = 0$

The auxiliary spectrum contains the value of the μ_j at the boundary $x = 0$. The oscillation modes must vanish at both ends of the interval $x_0 \in [0,L]$. Osborne and Segre (1993) describe an efficient method of integrating the Schrödinger equation to find the elements of the monodrony matrix Θ. Variation of E permits the graphical inspection of the Floquet discriminants for the main and auxiliary spectrum (see for instance Figure 5.1). The algorithm also stores the intermediate values $\Theta_{21}\,(x_0)$ during the integration. For $E = \mu_j$ satisfying the criterion $\Theta_{21}\,(x=L) = 0$, the stored value contains the oscillation mode value, $\mu_j\,(x_0) = \Theta_{21}\,(x_0)$
The oscillation modes are bounded between the eigenvalues of the main spectrum (E_{2i} and E_{2i+1}). The auxiliary spectrum condition is satisfied for a value of E lying between E_{2i} and E_{2i+1}, the eigenvalues of the main spectrum.
The Floquet diagram is constructed by varying E. The trace of the monodromy matrix equals 1 or -1 for an eigenvalue. The eigenvalues E_{2i} and E_{2i+1} are the eigenvalues corresponding to (soliton) mode i. The width of the band between these values determines the amplitude η_j of the oscillation mode:

$$\eta_j = \frac{E_{2j+1} - E_{2j}}{2\lambda} \quad (13)$$

Analogous to the Nyquist cutoff for Fourier series, there is a cutoff wavenumber for DPIST. This is the maximum wavenumber that can be found in a discrete signal and is determined by the number of discrete data points, $k_{\text{cutoff}} = \frac{\pi}{\Delta x}$, where k is the wavenumber defined by $k^2 = E$.

2.4 Inverse scattering problem: reconstruction

Once the μ_j's are integrated from a set of coupled ordinary differential equations, a summation of the rescaled μ_j's reconstructs the original signal completely. If desired, nonlinear filtering can be accomplished by omitting or altering some oscillation modes of the spectrum.

$$\begin{aligned} \lambda\eta(x,t) &= -E_1 + \\ &\quad \sum_{j=1}^{N}(-1)^{j+1}[2\mu_j(x,t) - E_{2j} - E_{2j+1}] \end{aligned} \quad (14)$$

The μ_j's lie on a two sheeted Riemann surface with branch points at E_{2j} and E_{2j+1}. As a band edge is approached, the derivative with respect to the horizontal coordinate of the oscillation modes changes sign. The factor $(-1)^{j+1}$ guarantees that the functions start off with the correct sign.
By omitting modes it is possible to filter the signal or find the soliton components in a certain signal. [Osborne *et al.*; Osborne et al. (1991)] have applied this technique on shallow water ocean surface waves. They

were able to extract the underlying soliton spectrum from a seemingly random signal.
The μ_j's interact during their evolution in time. However, when solitons are absent from the signal the interactions are weak. One can then assume that the functions evolve independently in time. Candela (1995) computed a set of eigenfunctions and a vector that governs the time evolution. Under the independence assumption, the signal could be reconstructed for all times. In general, however, reconstruction is complicated due to strong coupling of the μ_j's during their evolution.

3 Implementation of the numerical algorithm

The DPIST algorithm has been implemented in C^{++}. Validation studies have been performed on the computer program. The first test is to find the scattering transform of a single $sech^2$ soliton, an analytical solution of the KdV equation. The second test is of the time-invariance of the scattering power spectrum of a waveform propagating according to the KdV equation. A sine wave is evolved according to the KdV equation. It breaks up into solitons. The scattering power spectra are given at various times to verify the time-invariance property.

3.1 Simple soliton

A pure $sech^2$ shape oscillation mode can only be found when the potential is a single KdV soliton. This is not, in general, the case so the auxiliary spectrum of oscillation modes should contain both solitons (not quite $sech^2$ single humps due to the discrete and periodic approximations) and periodic cnoidal waves. The Floquet spectrum can be split in two parts. Imaginary and real wavenumbers k, each indicate an oscillation mode with a different form.
When there is no baseline shift in the potential, the soliton spectrum can be found for negative eigenvalues, i.e. imaginary wavenumbers. The shape of the Floquet spectrum reveals whether an eigenfunction is a soliton or a periodic cnoidal wave. The property I is computed by:

$$I = \frac{E_{2i+1} - E_{2i}}{E_{2i+1} - E_{2i-1}} \tag{15}$$

When the Floquet spectrum is very steep the property I will be between 0.99 and 1.0. This indicates the presence of a soliton. In general the soliton part of the spectrum is found for negative eigenvalues. Periodic solutions have values $I \ll 1$ and are found in positive eigenvalues. The soliton part of the spectrum is called the discrete spectrum. Periodic solutions are found in the continuous spectrum.
The shift in baseline of the signal can easily be found in the Floquet spectrum by replacing $\lambda u + k^2$ in (10) by $\lambda u + \lambda\overline{u} + k^2$, where $\overline{u}$ is the increase in amplitude due

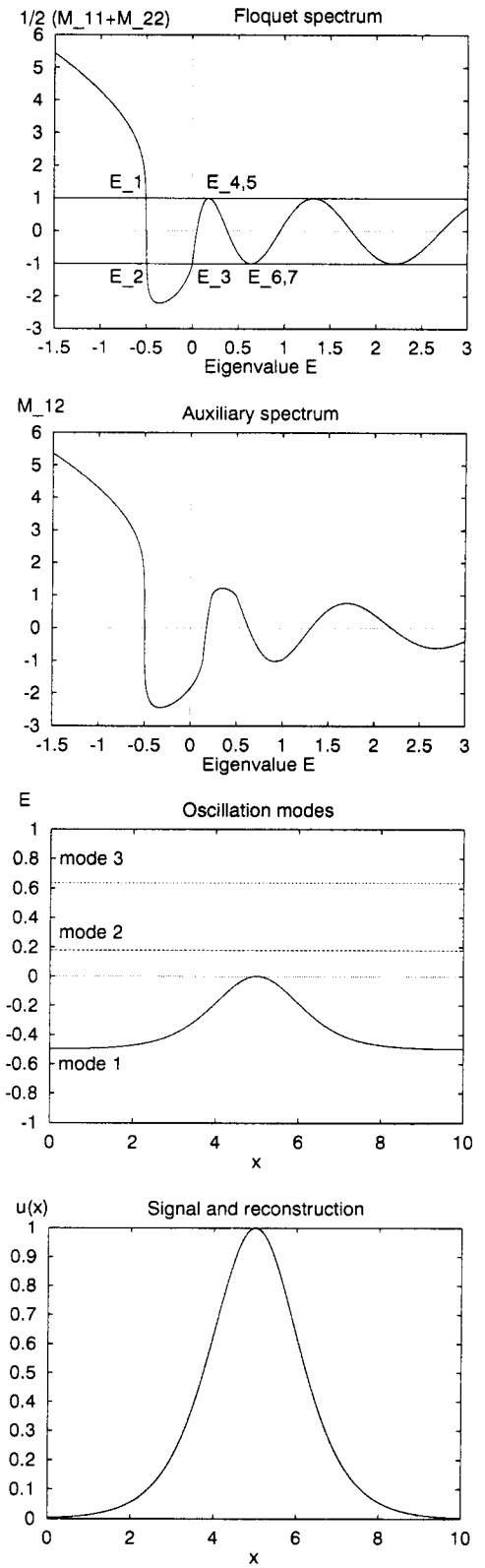

Fig. 1. Direct and inverse scattering transform of a solitary wave. Top: the Floquet spectrum, Next: the auxiliary spectrum, Next: the hyperelliptic oscillation modes, Bottom: the original potential (unbroken line) and the reconstructed potential (dashed line).

to the reference level. A baseline shift in the the signal ($\overline{u}$) will merely produce a shift $\lambda\overline{u}$ in the eigenvalues.
In Fig. 1 a pure soliton taken as the potential. The soliton $u = \frac{c}{2}\mathrm{sech}^2\left(\frac{\sqrt{c}}{2}(x-5.0)\right)$ is a solution to (5). The parameter c is chosen to be 2. The parameter λ is exactly unity in this case.
In the Floquet spectrum, Fig. 1A, the band width of the open gap between the values E_2 and E_3 determines the amplitude of the first mode. Theoretically there should be only one (soliton) solution present in this spectrum. In Fig. 1A and C it is clear that the solutions for mode 2 and 3 have negligibly small amplitude. The Floquet spectrum oscillates between +1 and -1 for all further values of E.
In Fig. 1A the zero crossings correspond to eigenvalues of the main spectrum. There is an auxiliary spectrum (Fig. 1B) between each successive pair of main spectrum eigenvalues E_{2i} and E_{2i+1}, and the oscillation modes oscillate between this pair. The corresponding auxiliary spectrum eigenvalue for mode 1 is situated between E_2 and E_3, for instance. This eigenvalue is used to compute the hyperelliptic oscillation modes of Fig. 1C. The original signal can now be reconstructed by linear superposition in Fig. 1D and is found to be superimposable with the original using only the seven modes of Fig. 1A, with all but the first negligible.
Up to the approximations made, the $sech^2$ waveform is recognised by DPIST as a solution of the KdV equation.
In the following sections the scattering transform is applied to the simulations and experiments. Periodicity of the signal will prove to be an important constraint on the applications.

3.2 Evolution of a sine wave

The evolution of an arbitrary periodic signal according to the KdV equation should produce a constant scattering power spectrum. When a linear sine wave ($\sin(x)$) is evolved in the spatial interval $[0, 2\pi]$ with coefficients $\alpha = 60$ and $\beta = 1$ (therefore $\lambda = 10$) it is expected that the signal will breakup into a train of solitons. The evolution of the sine wave is given in Fig. 2a. The Floquet spectrum of the sine wave is given in Fig. 2b.
The Floquet spectrum identifies four solitons and a large amplitude dispersive wave (number 5). In the evolved data in Fig. 2a, four clear solitons can be distinguished together with a small fifth wave. The Floquet spectrum in Fig. 2b identifies five nonlinear modes. There is a reasonably good agreement between the DPIST analysis, identifying solitary waves, and those seen in the data.
More detailed information on the time evolution of the sine wave is given in Fig 3. On the bottom plane a projection of the contour levels is made. The wave breaks up into a seemingly random profile of interacting waves, though completely deterministic. The individual solitons interact with other solitons and dispersive waves. From the contours projected at the lower surface it is clear that the waves continuously vary in amplitude and experience phase shifts. Despite these interactions the solitons retain their form.

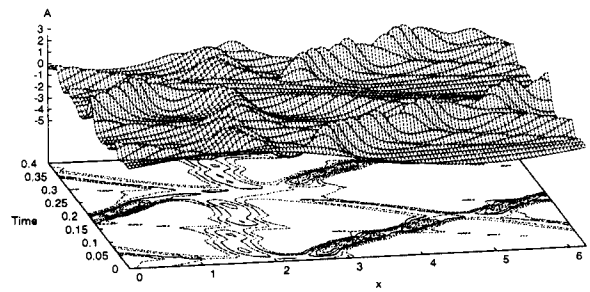

Fig. 3. Amplitude evolution of an initial sine wave according to the KdV equation.

The scattering power spectra at three different times in the simulation are given in Fig. 4. The power spectrum remains fairly constant in time. The variation may be accounted for by inaccuracies in the integration of the KdV equation and the discretization of the scattering transform. The power spectra is sufficiently time-invariant of the motion, a validation of the coding of DPIST used here.

4 Application of DPIST to simulations

The DPIST algorithm is applied to recent simulations of the dynamics of dense disturbances in stable stratifications which decompose into large amplitude internal gravity waves. The aim of this section is to test whether the wave evolution found is governed by the KdV equation and whether DPIST provides utility for the spectral analysis of the datasets.

4.1 Simulations

The computational fluid dynamics simulation scheme is described in detail in Haarlemmer (1997), Haarlemmer and Zimmerman (1996) and in the Appendix of Haarlemmer and Zimmerman (1999). Due to brevity concerns neither the finite volume implicit differencing technique nor the model system of partial differential equations appropriate to the simulation of a laminar atmosphere is reproduced here.
We have been developing atmospheric simulations of a 2-D domain under idealized conditions as a first approach to many open questions of localized releases of dense fluids in stable stratifications. Some of these releases develop into solitary wave disturbances. The physical applications include toxic gas accidental releases, chem-

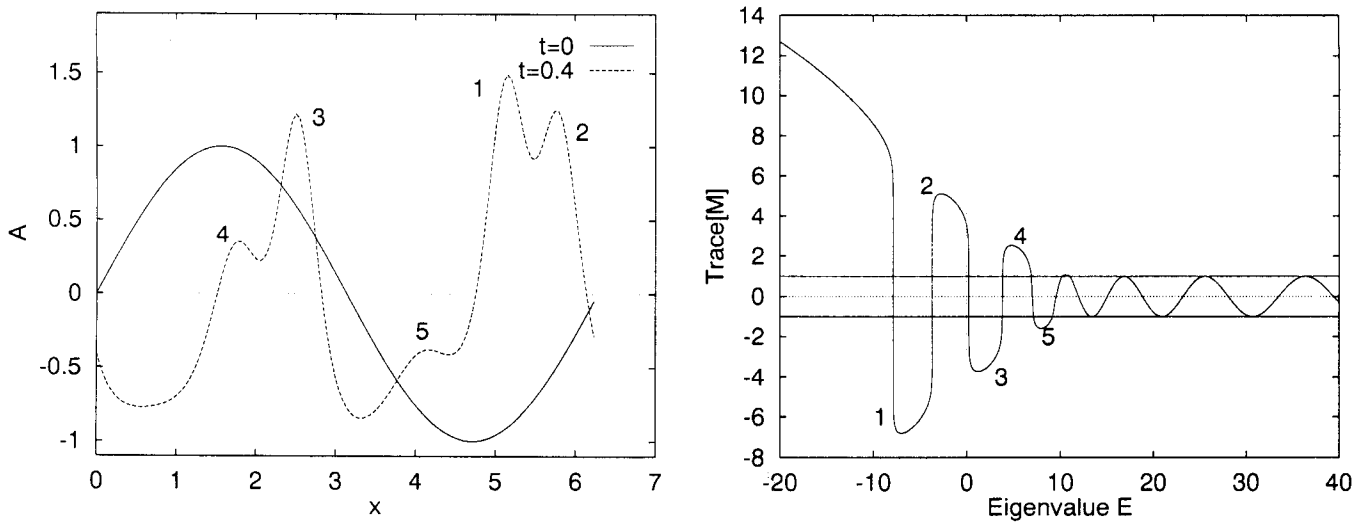

(a) Evolution

(b) Floquet spectrum

Fig. 2. (a): Sine wave evolved according to the KdV equation. (b): Floquet spectrum with five nonlinear modes identified. The numbers 1-4 identify the soliton spectrum, due to the threshold of $I \approx 0.99$ and number 5 is clearly less steep but still a large amplitude dispersive wave. Subsequent oscillation modes have negligible energy.

ical and biological warfare defense, and pollutant dispersal in atmospheric inversions or oceanographic thermoclines and pcynoclines. The first case studies have been reported in the fluid mixing literature in absence of wind shear [Haarlemmer and Zimmerman (1996)] with an initiation scheme that tweaks the velocity vector of an isolated neighbourhood of grid points. This artificial procedure is especially useful for generating "clean" solitary waves, whose wave dynamics and advecting ability can be closely monitored [Haarlemmer and Zimmerman (1999)] .

In [Zimmerman and Haarlemmer (1999)], we were concerned with relieving the ideal initiation by creating an initial disturbance which is both a mass (temperature) and momentum source at the inlet of the domain. These dynamic inlet conditions, performed with a variety of waveguides, permit the study of the effects of generation mechanisms, different wave sizes, stratifications, and the background wind profiles on the wave evolution.

Simulations were performed with either a uniform background velocity or a sheared background. Temperature profiles are only stratified near the bottom surface and left unstratified above 300m. Several types of wave events were simulated. The stratification and the initial disturbances were varied throughout [Zimmerman and Haarlemmer (1999)].

Waves were created by blowing a transient cold gust into the waveguide. The scenario is similar to that described in Doviak and Christie (1991). They explain how a thunderstorm downdraft can create a train of solitary waves. Other situations where this mechanism may trigger a solitary wave is an explosive release of a cold gas (e.g. rupture of a tank containing liquid gas) or a sea breeze flowing into a nocturnal inversion layer (gravity current). The origination of waves is influenced by the wind which interacts with the gust. Once the wave develops, the effect of the uniform wind should be negligible.

The simulations describe the creation of solitary disturbances and their evolution in time. A packet of cold air is released creating a perturbation in the temperature profile and streamlines. No attempt was made to resolve the fine scales of the jet flowing into the stratification. After the initial burst settled down the accuracy increased. The size of the mesh is 40km (200 grid points) by 1000m (50 grid points) and the size of the time steps is 20s. The background wind is set to be either uniformly at 5m/s [Haarlemmer and Zimmerman (1996); Haarlemmer and Zimmerman (1999)] or sheared [Haarlemmer (1997)].

All of the kinetic energy added is initially localized and then spreads out and evolves into a solitary wave. Potential temperature profile A is linearly stratified from 10 to 11 °C in the lower 300m, the upper unstratified layer is set to 11°C (Brunt-Väisälä frequency $1.0 \cdot 10^{-2}$ s^{-1}). Potential temperature profile B is linearly stratified from 10 to 14°C (Brunt-Väisälä frequency $2.2 \cdot 10^{-2}$ s^{-1}) and left unstratified above. The various simulations presented here are listed in Table 1.

4.2 Simulation 1: Falling Dense Disturbance

The simulations in Chapter 5 of Haarlemmer (1997) initiate from a turbulent region from which solitary waves

Table 1. Numerical simulations performed in this paper, with the amplitude amp [m] of the initial disturbance and the particularities of the simulations. () is the time at which the amplitude is measured. v [m/s], time [s], and T[°C] refer to the velocity, duration, and temperature of the initial cold air gust.

No	type	v	time	T	amp	ε	reference
1	B	-50	40	10	111 (400)	0.39	Haarlemmer (1997) Sim. 5.2
2	B	20	40	10	129 (800)	0.43	Haarlemmer and Zimmerman (1999) Sim. 3

emanate. These waves are initially highly nonlinear. As their amplitude decreases they slowly evolve into weakly nonlinear waves.
In this simulation the fluid was linearly stratified in the first 300m with temperature increasing from 10°C to 14°C. The top layer was left unstratified at 14°C. A wave was created close to the left boundary by setting a region with a local vertical velocity to 50 m/s, directed downwards. A part of the fluid near the origin of the wave was labelled with a tracer with concentration unity. The mesh is 10km in the x-direction (100 grid points) and 1km in the y-direction (50 grid points).
The wave that is analysed is the perturbed location of the 13.8°C isotherm and is therefore near the top of the stratification. This isotherm is given in Fig. 5a for different times. It is clear from this graph that the signal is not periodic. The data was edited in Fig. 5b to isolate the wave of interest and insure periodicity of the data. The scattering algorithm was applied to the data in Fig. 5b. The coefficients of the nonlinear and dispersive terms are given by Benney (1966). In dimensionless form these take the values $\alpha = \varepsilon * 5.5$ and $\beta = \mu^2 * 0.032$. This gives a value for the nonlinearity parameter as defined by (4) as a function of the wave parameters:

$$\lambda = \frac{\varepsilon}{\mu^2} \cdot 29$$

The horizontal characteristic length scale is chosen to be identical to the vertical scale, thus $\mu = 1$. First the scattering transform is applied to the data at t=800s. At this time $\varepsilon = 0.1$, resulting in $\lambda = 2.9$. The wave at each time is normalised to unity to assure that the non-dimensional form of the KdV equation as derived by Benney is used. The results of the scattering transform are presented in Fig. 7. The reconstruction of the wave signal is imperfect. However, given how few modes are employed (7 modes) the reconstruction can be considered reasonable. From the Floquet spectrum and the first four oscillation modes it is clear that there is one dominant soliton present in the data. This is what could be expected from Fig. 5b.
The scattering transform is applied to the data at t=1200s ($\lambda = 2.5$) and t=1600 ($\lambda = 2.2$). The three power spectra are compared in Fig. 8. The overall power spectrum remains fairly constant in time. It is however not an invariant of the motion. The leading mode steadily decreases in amplitude. Apparently there is a mechanism that transforms the leading wave, decreasing its amplitude and increasing its support. Dispersion is the most likely mechanism for this behavior. The simulations, however, contain bulk viscous dissipation appropriate to the atmosphere, which is expected to have minimal effect. More realistic turbulent eddy viscosity was omitted for simplicity. The Fourier power spectrum needs many more modes to describe the signal. This is due to the non-localised character of the transform. The Fourier power spectrum is clearly more variable in time than the scattering power spectrum.
The scattering transform can also be applied to the full dataset as presented in Fig.5a. It is expected that the modes present in the modified data are also found in the full data. The scattering power spectra for the full data are given in Fig. 9. Initially the spectrum changes in time, however after some time in the simulation the spectrum remains fairly constant. The leading mode decreases in amplitude similarly as in Fig. 8.
From this study we can conclude that the scattering transform is a suitable analysis tool for this wave data. It can identify modes that remain constant throughout the motion, if there are any. It is necessary, however, to use the proper scales of the waves in the scattering equations.

4.3 Simulation 2: Rising Dense Disturbance

The simulations in [Haarlemmer (1997); Haarlemmer and Zimmerman (1996); Haarlemmer and Zimmerman (1999); Zimmerman and Haarlemmer (1999)] have been shown to produce waves that are very efficient in the transport and convection of fluids. This was due to the fact that the waves are relatively large and display non-similar disturbance streamlines at different heights. The weakly nonlinear assumption is strictly speaking not valid in these simulations.
Simulation 2 differs from 1 by introducing the dense disturbance in the inlet of the domain with positive vertical velocity, rising rather than falling, for a given period, thus introducing more disturbance energy. A disturbance was released with a velocity of 20m/s for 40s (temperature 10°C, concentration tracer unity). This creates a wave with an amplitude of 129m (after 400s). The scattering transform was applied on the wave data derived from the location of the 13.8°C isotherm. The wave data is graphed in Fig. 6a. The temperature stratification in this simulation is the same as in section 4.2. The wave amplitude decreases after an initial increase.

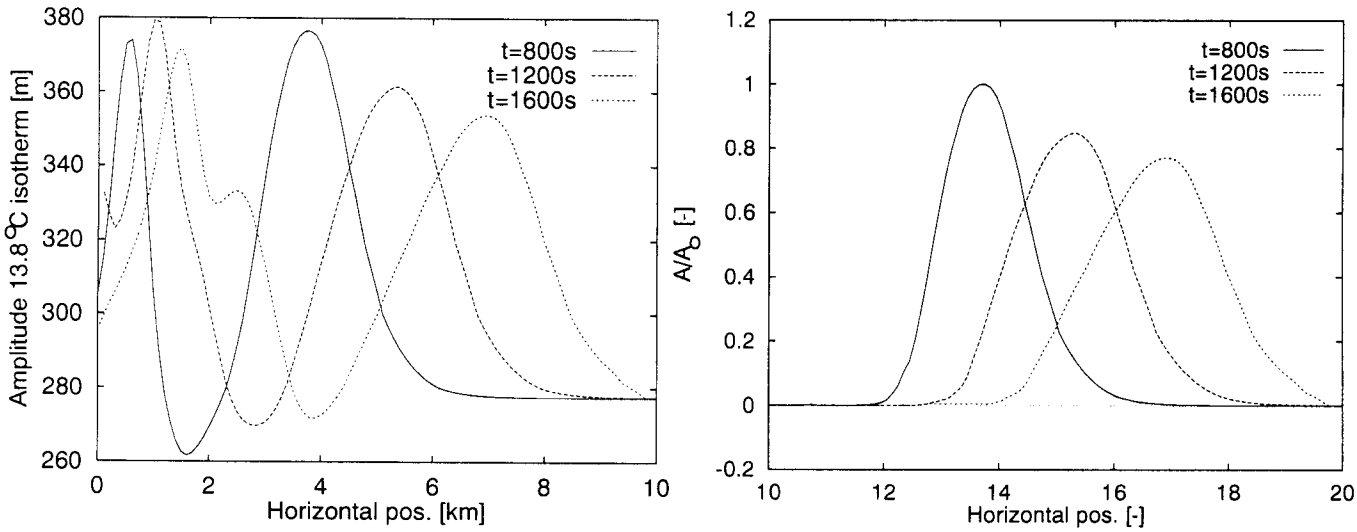

(a) Raw data

(b) Solitary wave isolated

Fig. 5. (a): Location of the 13.8°C isotherm of simulation 1. (b): Solitary wave isolated to insure periodicity and made dimensionless by the amplitude of the initial wave.

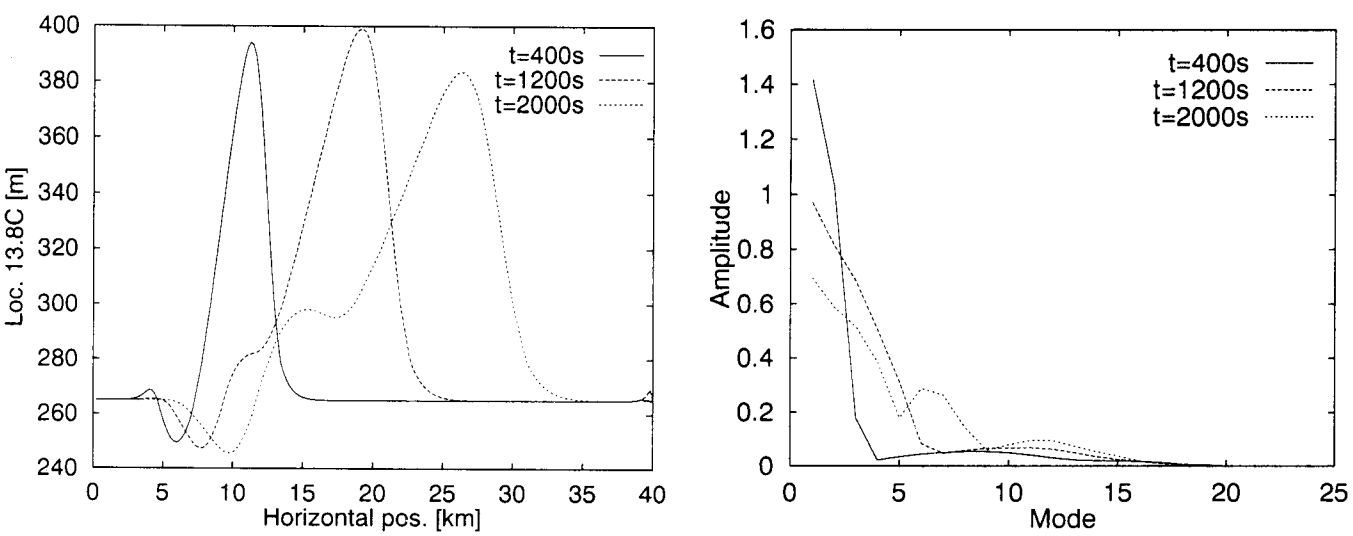

(a) Wave data

(b) Scattering power spectra

Fig. 6. (a): Location of the 13.8°C isotherm in simulation 2. (b): Scattering power spectra.

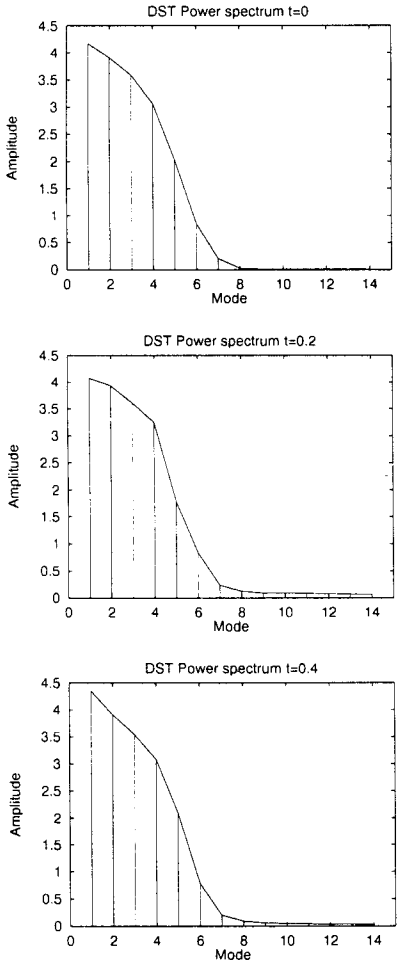

Fig. 4. Scattering power spectra of the wave evolution in Fig. 4 at three different times.

The value of λ varies from λ=3.8 at t=400s, λ=4.1 at t=1200s to λ=3.5 at t=2000s. This is reflected in the scattering power spectra in Fig. 6b. The power spectra are represented in one graph for easy comparison.
The signal is clearly not governed by the KdV equation because the power spectrum varies considerably. Various reasons can be given for this failure. Dissipative effects can play an important role in the wave evolution. Alternatively the weakly nonlinear assumption that the wave separates fails, i.e. the disturbance does not take the same form on every streamline.

4.4 Discussion

The results presented here assume that the KdV coefficients change with the wave under study. Benney (1966) assumed a long wave form and derived the KdV equation for this wave. The assumptions implied that as the wave evolves, so does the governing equation. If the wave data from the simulations is analysed using the inverse scattering transform it is suggested that the wave

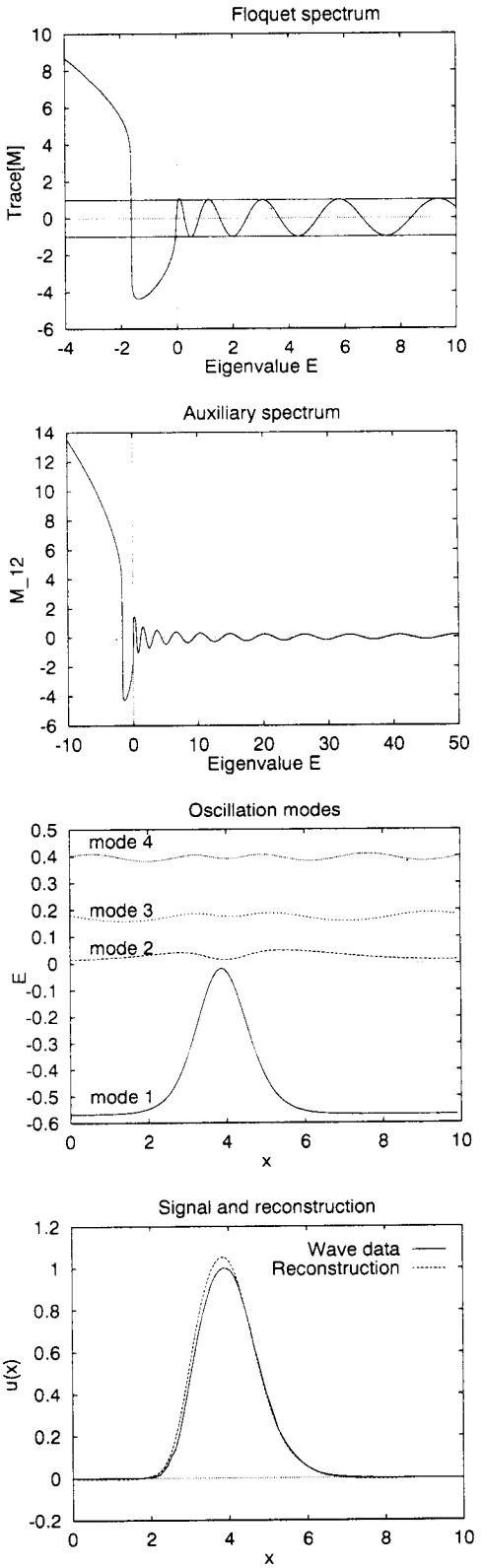

Fig. 7. Inverse Scattering Transform of the wave data of simulation 1. Top: the Floquet spectrum, Next: the auxiliary spectrum, Next: the hyperelliptic oscillation modes, Bottom: the original potential (straight line) and the reconstructed potential (dashed line).

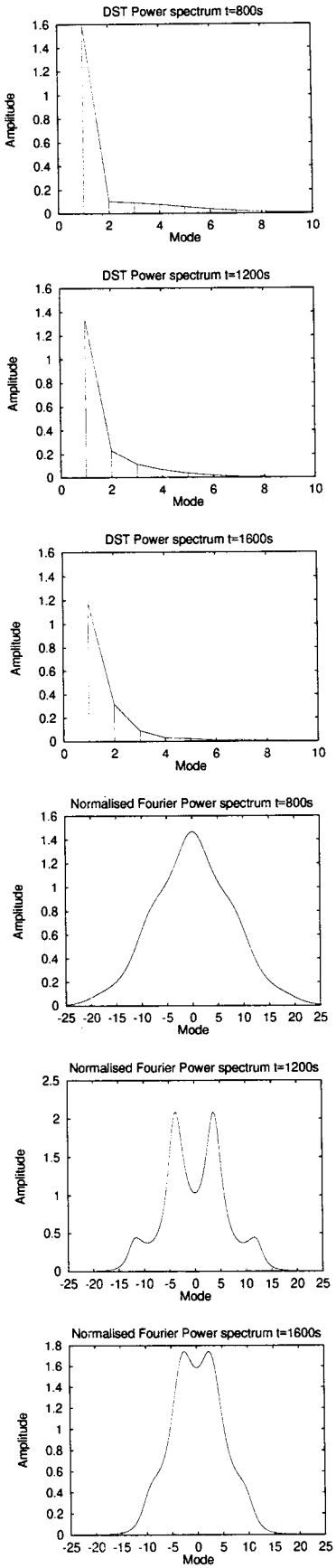

Fig. 8. Power spectra of the modified waves in Fig. 5. The Fourier power spectrum are calculated by the maximum entropy method.

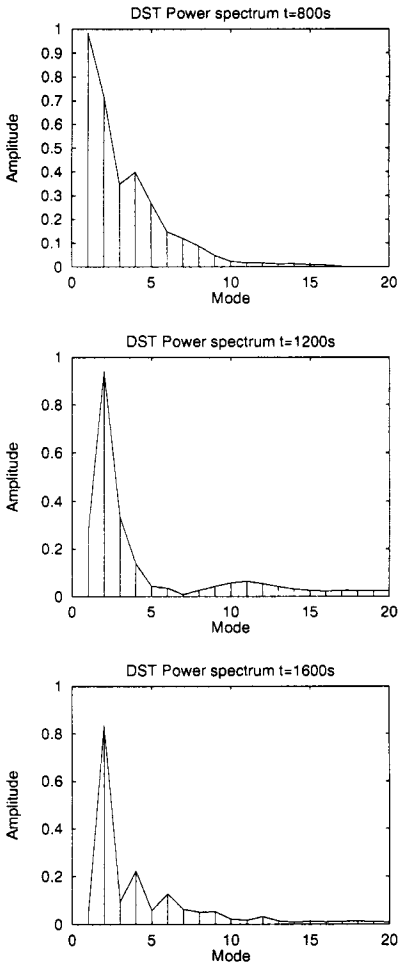

Fig. 9. Scattering power spectra of the unmodified waves in Fig. 5.

motion sometimes is governed by KdV equation with selected λ. It is found that the wave must be separable and relatively clean of dispersive waves for the power spectrum of the scattering transform to be an invariant of the motion.

In section 4.2 it was shown that the power spectrum of one isolated wave is not necessarily present in the power spectrum of the full wave data. Due to nonlinear interactions between the modes, power spectra cannot be superimposed.

Unfortunately this implies that little predictive value can be attached to the scattering transform for internal waves. One needs more information about the wave to analyse it. This information is specific to a chosen wave, typically the leading largest amplitude wave. The scattering parameter λ is then incorrect for other smaller waves. This may account for the observations that there is at maximum only one constant mode in the simulations.

Furthermore the scattering transform does not identify a specific soliton that evolves from an arbitrary signal.

Due to nonlinear interactions between the hyperelliptic oscillation modes, the modes evolve strongly coupled in time.

5 Application of DPIST to experiments

The scattering transform can be applied to experimental wave data. Wave experiments were performed as described in Haarlemmer (1997) Chapter 7. The wave tank in which the experiments are done was purpose built. The tank is a rectangular channel made of transparent U-PVC. The dimensions are $200 \times 25 \times 10$cm. Data is collected using conductivity probes and a video camera. The results are presented in the form of conductivity probe readings and video stills.
A stratification is set up by introducing fluids of different densities in the tank. First fresh water is put in place after which batches of brine with increasing densities and different colours are introduced near the bottom of the tank. The different fluids organise themselves vertically with the lightest fluid on the top. The interfaces are miscible and so a near linear stratification can be set up with a known density distribution.
The wave data was collected using conductivity probes and a data acquisition system. The conductivity probes are fed with an AC-current and the voltage drop referenced to a system of known resistance is logged by a computer. Data was taken every 50ms.
The datasets collected using conductivity probes were conditioned as follows. The probe signal was calibrated using the wave amplitude of observed from the video stills. Electronic noise was reduced by using a low pass filter.
It is possible to generate solitary waves in a great many ways [Amen and Maxworthy (1980), Maxworthy (1979)]. Almost any disturbance in stably stratified fluids produces waves of some sort. Gravity currents are created by an area of fluid with a high density separated from the stratification. When the separation is removed the dense fluid flows into the stratification creating a train of solitary waves (see also Maxworthy (1980) and Rottman and Simpson (1989)). In most experiments conducted in our studies a localised solitary wave is created by introducing a small but finite volume of dense fluid in the stratification. This results in a solitary wave without generating a gravity current.
Various experiments have been performed with different density stratifications. Both shallow and deep water situations are considered. The experiments for this section are presented in the form of video stills. A finite amount of dense fluid (typically 100ml) was introduced in the stratification. This causes a negligible increase in the fluid level (0.5mm).

5.1 Deep fluids

In the first experiment in this section a wave was created on a stratification embedded in a relatively deep fluid. The wave was created using the method described above. A solitary wave was generated that propagated though the stratification. Due to the fact that the wave travels very slowly, viscous forces damp the wave. The waveforms generated in this study were damped and usually disappeared after two passes in the tank.
The video stills of experiment 1 are shown in Fig. 10. The figure clearly shows a solitary wave propagating with very little change of form during eight seconds. The coefficient λ in the scattering equations is computed in the same way as described in section 4.2. On the basis of the dimensionless coordinate system, where the amplitude is scaled by the maximum amplitude of the wave A_0 and the horizontal position is scaled by the fluid height, λ is given by:

$$\lambda = \varepsilon \cdot \frac{\alpha}{6\beta} = \varepsilon \cdot 77.9$$

The wave form found in this experiment is given in dimensionless form in Fig. 11. The wave data was found from processing the video images. It is clear that the same mechanisms are at work as in the simulations. The wave decreases in amplitude and increases in wave length. The value for λ varies from $\lambda = 20$ initially to $\lambda = 17$ after 8s.
The results in Fig. 11 clearly show that the wave is not completely governed by the KdV theory. Although the power spectra show that there is one mode that remains fairly constant, it appears that all other modes slowly disperse and dissipate and that only one nonlinear mode survives. The initial signal is reconstructed with the four oscillation modes as shown in Fig. 11. The results shows that the scattering transform provides an efficient method of describing the signal.

5.2 Shallow fluids

The second experiment which is analysed with the scattering transform deals with a more shallow fluid. The wave data was taken from the video stills as presented for experiment 1 in Chapter 7 of Haarlemmer (1997). The value of the parameter is $\lambda = \varepsilon \cdot 13.4$. Length scales are scaled by the height of the waveguide. The results of the scattering transform are given in Fig. 12.
The scattering power spectrum is roughly constant in time. The wave data of this experiment is not of very high quality so some discrepancy can be expected. The times between the two waveforms is only a few seconds so only small changes in the power spectrum can be expected.

Exp. No	Stratification		Description
	Depth Layer [cm]	Density [kg/m^3]	
1	10	1,000	Wave created by introducing 100ml dyed fluid, density 1.04kg/m^3.
	2	1,008	
2	4	1,000	Wave created by introducing 100ml dyed fluid, density 1.05kg/m^3.
	1	1,008	
	1	1,015	
	1	1,023	

Table 2. Experiments performed in this paper.

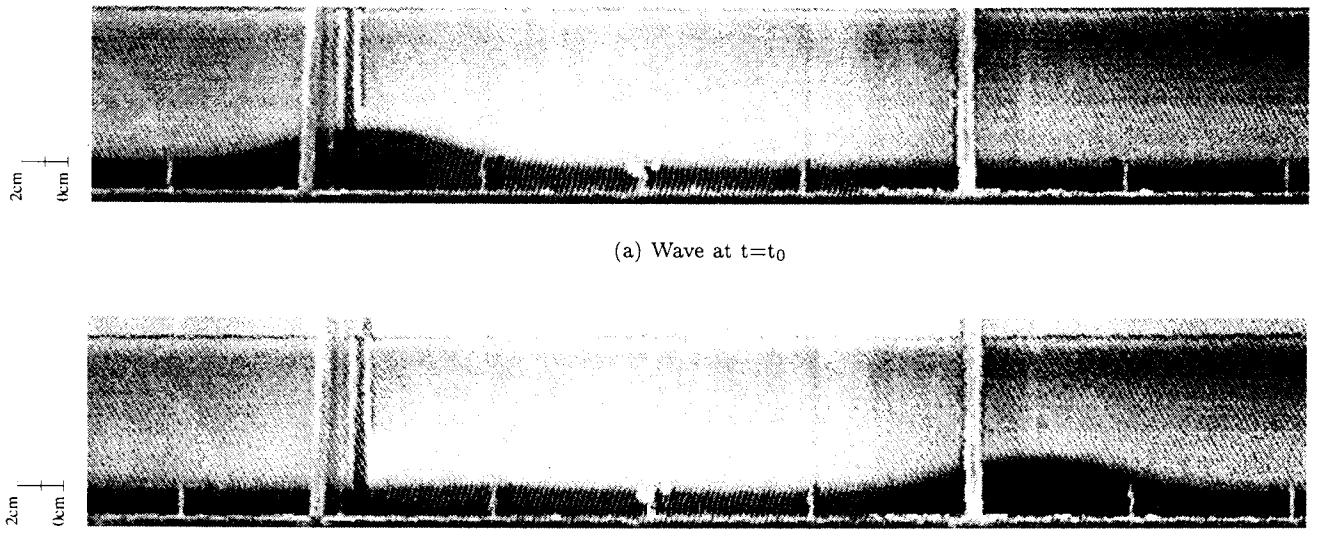

(a) Wave at t=t_0

(b) Wave at t=t_0+8s

Fig. 10. Video stills of experiment 1, 80cm section of the wave tank, 20cm from the origin of the wave.

5.3 Discussion

The application of the scattering transform to the experimental data show that the arguments found in section 4 still hold. The size of the wave varies and therefore the coefficients vary. When variable coefficients are used the data appears to be consistent with the KdV equation. Waves in weakly viscous fluids can be described approximately by using the inviscid equations. Most experiments however deal with pseudo-steady situations with a small but finite initial input of energy. Alternatively for surface waves the weakly viscous approximation may be applicable due to the short time scales involved. The experiments performed in this study show that the time scales for internal waves are much longer and viscous forces act on the motion. The first modes to be damped however are the smaller dispersive modes. The leading soliton components of the data survive for some time.

6 Concluding Remarks

It is possible to treat internal wave data from various sources by DPIST analysis. Other researchers as yet have only analysed surface wave data with the scattering transform. The nature of the perturbation expansions deriving weakly nonlinear evolution equations for internal waves is different than those for surface waves. The implementation of the scattering algorithm had to be adapted to the use on internal waves.

It was possible to identify constant wave modes in some of the simulations and experiments presented in this paper. A prerequisite for this is, however, that the wave is separable and weakly nonlinear. Strongly nonlinear waves that do not separate have a scattering power spectrum that varies with time.

As has been shown, the KdV coefficients, and thus the input parameter $\lambda = \frac{\alpha}{6\beta}$ for DPIST analysis depend on the characteristic amplitude and wavenumber through the Ursell number $\mathrm{Ur} = \frac{\varepsilon}{\mu^2}$ for both internal and surface waves. Additionally, λ depends on the profiles $\hat{u}(z)$ and $\hat{\rho}(z)$ forming the waveguide for internal waves. Thus, for geophysical flows in a stably stratified, sheared shallow fluid layer, measurements of the background conditions and the wavelength and the amplitude of a solitary wave passage must be performed for DPIST to have a predictive value. Very few studies qualify. Rees and Rottman

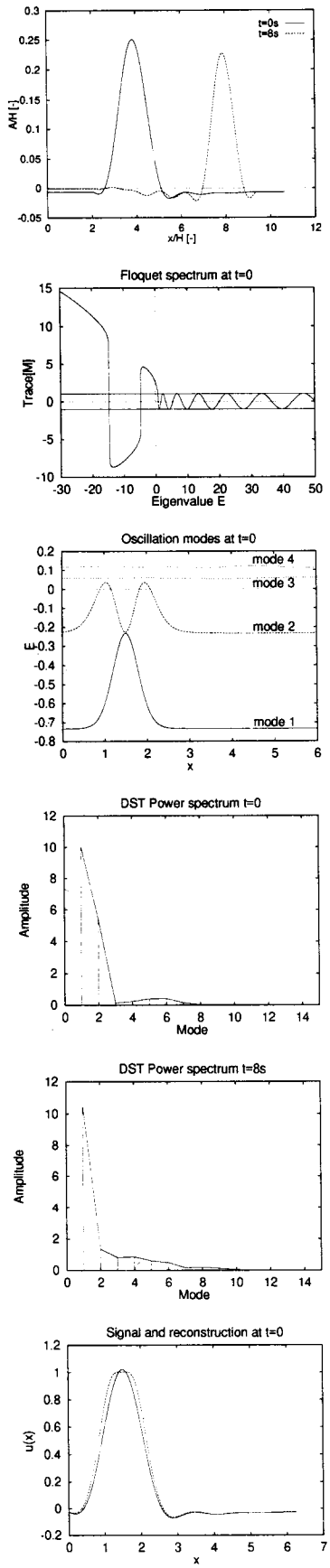

Fig. 11. Scattering data of the waves in Experiment 1.

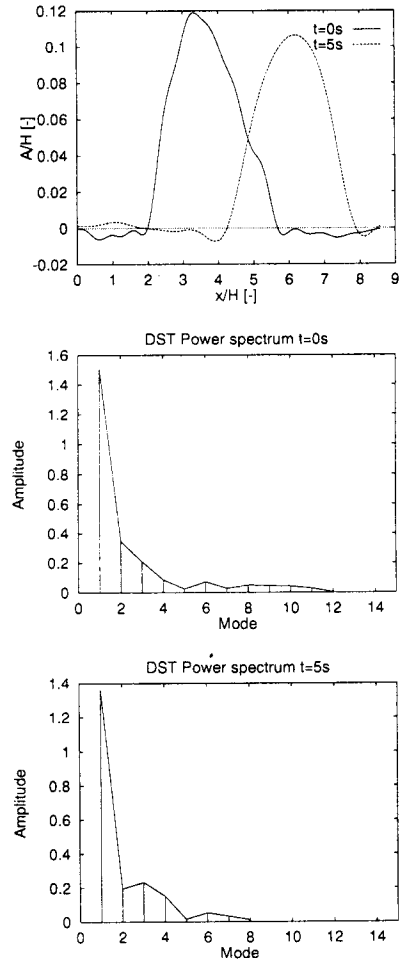

Fig. 12. Scattering data of the waves in Experiment 2.

(1994) reported large amplitude solitary waves propagating over an Antarctic ice shelf during the stably stratified austral winter of 1986. Sufficient information is present to use DPIST for prediction, but measurements are not taken downwind for validation.

Alternatively, for DPIST to have predictive value for internal wave propagation, the background conditions must be such that a class of waves with prescribed wavenun ber and amplitude are generated or selected. Three such situations come to mind:

1. Zimmerman and Rees (1997) propose a theory that when the Scorer parameter [Scorer (1949)] is locally positive in a stratum embedded in a stable atmospheric inversion, (for instance if a low level jet opposes a unifom stream) then nearly monochromatic long waves in a wave packet strictly greater than the Scorer wavenumber are trapped in the waveguide and associated with the largest amplitude component. Under the steady wave assumption in the frame of reference of the long wave linear phase velocity, there is an unique amplitude pre-

dicted for solitary waves with the Scorer wavenumber, i.e. fixed λ. Faster moving solitary waves with amplitude linked to the phase velocity are also solutions to the weakly nonlinear wave equation derived, a hydrid of the KdV and BBM [Benjamin et al. (1972)] equations. Hypothetically, DPIST could be used as a predictive analysis tool under these conditions.

2. Velarde and coworkers (see e.g. Nepomnyashchy and Velarde (1994) for the derivation and Christov and Velarde (1995) for some dynamical behavior of the nonlinear evolution equation) have demonstrated that surface solitary waves and thus slaved internal gravity waves can be generated in the Marangoni-Benard venue when heated from above – the air side of the air-liquid interface. The solitary waves are excited above a threshold in Marangoni number with amplitude and wave-number dependent on the excess Marangoni number above the threshold. The dynamics are shown to satisfy the modified KdV equation dubbed the KdV-KSV equation, including the dissipative terms usually associated with the KS equation. Under certain restrictions of the coefficients, this dissipation modified KdV equation is integrable [Lou et al. (1991); Estevez and Gordoa (1993); Cerveró and Zurrón (1996)] and thus a DPIST exists. How robust this DPIST analysis tool is for the in general, non-integrable KdV-KSV equation is an open question.

3. Zimmerman and Velarde (1996) derive a variant of the KdV-KSV for bulk dissipative effects on the evolution of internal solitary waves by arguing that the center manifold dynamics of slow variations of the waveguide height and the least dissipated internal mode are dominant in the time-asymptotic limit. External wave energy input to the disturbance, for instance from shear instability, is necessary for solitary internal waves to propagate indefinitely. Under conditions of strong shear, it is likely that the shear instability sets the scale of the solitary wave.

This study has shown that when, as in the experiments of Osborne and Petti (1994) waves are generated with monochromatic wavenumber and controlled amplitude, DPIST is an exceptionally good spectral analysis technique. For internal waves, additionally, the waveguide must be well characterized. However, in the practical applications which generate solitary disturbances – in oceanography and meteorology, as well as pollutant dispersal and accidental toxic gas releases – the initial condition may be too strongly nonlinear for the KdV approximation to be valid. Nevertheless, the long time evolution of the solitary waves generated in shallow layers may approximate KdV dynamics. Fixing the key DPIST input parameter λ in these cases could be problematic. For simulations and wave tank experiments modelling these cases, it has been found that the DPIST spectral analysis identifies the largest amplitude solitary disturbance and its power spectrum under some uncertainty about the proper λ. Thus, the DPIST technique is promising as a nonlinear filter for the prediction of the propagation of single nonlinear dispersive internal waves.

Acknowledgements: The authors would like to thank the National Science Foundation and North Atlantic Treaty Organization for a postdoctoral fellowship (WBZ) and collaborative research grant, CRG 940242 and acknowledge helpful discussions with Professor M G Velarde of Complutense University of Madrid and Professor C I Christov of the Bulgarian Meteorological Institute, Sofia. The second author is grateful for a UMIST postgraduate fellowship. Use of the PHOENICS CFD engine is acknowledged.

References

Amen,R. and T. Maxworthy. "The gravitational collapse of a mixed region into a linearly stratified fluid." *J. Fluid Mech.*, 96:65–80, 1980.

Benjamin, T.B. "Internal waves of finite amplitude and permanent form." *J. Fluid Mech.*, 25:241–270, 1966.

Benjamin,T.B., J.L. Bona, and J.J. Mahony. "Model equations for long waves in nonlinear dispersive systems.". *Philos. Trans. Roy. Soc. London*, Ser. A 272:47–78, 1972.

Benney, D.J. "Long nonlinear waves in fluid flows." *J. Math. Phys.*, 45:52–63, 1966.

Candela, D. "Numerical methods for nonlinear Fourier analysis, prediction and filtering". *J. Comp. Phys.*, 117:205–214, 1995.

Cerveró,J.M. and O. Zurrón. "Integrability of the perturbed KdV equation for convecting fluids: symmetry analysis and solutions." *Nonlin. Math. Phys.*, 3:(1-2):1–23, 1996.

Christov,C.I. and M.G. Velarde. "Dissipative solitons.". *Physica*, D86:323–347, 1995.

Drazin, P.G. and R.S. Johnson. Solitons: an Introduction, Cambridge University Press, Cambridge, 1989.

Doviak, R.J., S.S. Chen, and D.R. Christie "A thunderstorm generated solitary wave observation compared with theory for nonlinear waves in a sheared atmosphere." *J. Atmos. Sci.*, 48(1):87–111, 1991.

Estevez,P.G. and P.R. Gordoa. "Generalized solutions of the perturbed KdV equation for convecting fluids." in *Applications of Analytic and Geometric Methods to Nonlienar Differential equations*, P.A. Clarkson ed., Kluwer Academic Publishers, Netherlands, pp. 287–288, 1993.

Ferguson, W.E., H. Flashka, and D. W. McLaughlin. "Nonlinear normal modes for the Toda chain". *J. Comput. Phys.*, 45:157 , 1982.

Fermi,E., J. Pasta, and S. Ulam. "Studies of nonlinear problems", LASL Report LA-1940 (1955), Reprinted in Collected Papers of E. Fermi, Vol II, Univ. of Chicago Press, pp 978-988, 1965.

Flashka, H. "The Toda lattice: II. Existence of integrals". *Phys. Rev. B*, 9(4):1924–1925, 1974.

Flashka, H. and D. W. McLaughlin, "Canonically conjugate variables for the Korteweg-de Vries Equation and the Toda lattice with periodic boundary conditions". *Prog. Theor. Phys.*, 55(2):438–456, 1976.

Gardner,C.D., J.M. Greene, M.D. Kruskal, and R.M. Miura.

"Method for solving the Korteweg-de Vries equation", *Phys. Rev. Lett.*, 19:1095–1097, 1967.

Gear, J.A. and R. Grimshaw. "A second-order theory for solitary waves in shallow fluids.". *Phys. Fluids*, 26(1):14–29, 1983.

Goldstein, S. "On the stability of superposed streams of fluids of different densities.". *Proc Roy Soc A*, 132:524–548, 1931.

Haarlemmer, G.W. "Dynamics of internal solitary waves in stable stratifications in ocean and atmosphere." *Ph. D. thesis*, University of Manchester Institute of Science and Technology, 1997.

Haarlemmer, G.W. and W.B. Zimmerman. "Enhancement of mixing by internal solitary waves in stratified flows." Mixing V, *I Chem E Symposium Series*, H. Benkreira ed. *140*:225-235, 1996.

Haarlemmer, G.W. and W.B. Zimmerman. "Advection of pollutants by internal solitary waves in oceanic and atmospheric stable stratifications." *Nonlinear Processes in Geophysics*, in press, 1999a.

Koop, C.G. and G. Butler. "An investigation of internal solitary waves in a two-fluid system.". *J. Fluid Mech.*, 112:225–251, 1981.

Korteweg, D.J. and G. de Vries. "On the change of form of long waves advancing in a rectangular canal, and on anew type of long stationary waves." *Philos. Mag* Ser. 5: 422, 1895.

Lamb, Jr., G.L. *Elements of Solition Theory*, Wiley - Interscience, New York, 1980, p, 118ff.

Long, R. R. "Solitary waves in the Westerlies" em J. Atmos. Sci. 21: 156, 1964.

Lou,S.-y., G.-x. Huang, and H.-y. Ruan. "Exact solitary waves in a convecting fluid." *J. Phys. A: Math. Gen.*, 24:L587-L590, 1991.

S.A. Maslowe and L.G. Redekopp. "Long nonlinear waves in stratified shear flows.". *J. Fluid Mech.*, 101(2):321–348, 1980.

Maxworthy, T. "A note on the internal solitary waves produced by tidal flow over a three dimensional ridge". *J. Geograph. Res.*, 84:338–346, 1979.

Maxworthy, T. "On the formation of nonlinear internal waves from the gravitational collapse of mixed regions in two and three dimensions". *J. Fluid Mech.*, 96:47–64, 1980.

Maxworthy, T. and L.G. Redekopp. "Theory of the Great Red Spot and other observed features of the Jovian atmosphere" em Icarus 29:261, 1976.

Nepomnyashchy,A.A. and M.G. Velarde. "A three-dimensional description of solitary waves and their interaction in Marangoni–Benard layers.". *Phys. Fluids*, 6(1):187–198, 1994.

Osborne, A.R. "Nonlinear Fourier analysis." in it Nonlinear Topics in Ocean Physics ed. A.R. Osborne, North-Holland, Amsterdam, 1991.

Osborne,A.R. and L. Bergamasco. "The small-amplitude limit of the spectial transform for the periodic, Korteweg-de Vries equation". *Nuovo Cimento* B85:2293, 1985.

Osborne,A.R. and L. Bergamasco. "The solitions of Zabusky and Kruskal revisited I: Perspective in terms of the periodic scattering transform." *Physica* D:18:26, 1986.

Osborne, A.R. and M. Petti. "Numerical inverse-scattering-transform analysis of laboratory-generated surface wave trains." *Phys. Rev.* E49:1035, 1993.

Osborne, A.R. and M. Petti. "Laboratory-generated, shallow-water surface waves: Analysis using the periodic, inverse scattering transform." *Phys. Fluids* 6(5):1727 1744, 1994.

Osborne, A.R. and E. Segre. "Numerical solutions of the Korteweg-deVries equations the periodic scattering transform μ representation" *Physica* D44:575, 1990.

Osborne, A.R. and E. Segre. "The numerical inverse scattering transform for the periodic Korteweg-de Vries equation". *Phys. Lett. A*, 173:131–142, 1993.

Osborne, A.R., E. Segre, G. Boffetta, and L. Cavaleri. "Solsis states in shallow-water ocean surfaces waves." *Phys. Rev. lett.* 64: 1733, 1991.

Peregrine, D.H. "Calculations of the development of an undular bore." *J. Fluid Mech.*, 25:321-330, 1966.

Rees,J.M. and J.W. Rottman. "Analysis of solitary disturbances over an antarctic ice shelf.". *Boundary-Layer Met.*, 69:285-310, 1994.

Rottman,J.W. and J.E. Simpson. "The formation of internal bores in the atmosphere: A laboratory model". *J. Roy. Met. Soc.*, 115:941–963, 1989.

Scorer, R. S. "Theory of waves in the lee of mountains.". *Quart. J. R. Meteorol. Soc.*, 75:41–56, 1949.

Taylor, G. I. "Effect of variation in density on the stability of superposed streams of fluid". *Proc Roy Soc A*, 132:499–523, 1931.

Weidman,P.D., and M.G. Velarde. "Internal Solitary Waves". *Studies in App Math*, 86:167–184, 1992.

Whitham, G.B. Linear and nonlinear waves. John Wiley & sons, New York, 1974, p.585ff.

Zimmerman, W.B. and G.W. Haarlemmer. "Tracer dispersion by internal solitary waves in stable stratifications." Mixing and Dispersion in Stably Stratified Flows, Proceedings of the IMA, New Series Number 68, 373–392, P.A. Davies, ed., 1999b.

Zimmerman, W.B. and J.M. Rees. "The wavelength of solitary internal waves in stable stratifications." *Phys. Fluids*, submitted, 1997.

Zimmerman,W. B. and M.G. Velarde. "A centre manifold approach to solitary internal waves in a sheared, stably stratified fluid layer." *Nonlinear Processes in Geophysics*, 3:110–114, 1996.

Zimmerman,W. B. and M.G. Velarde. "Strong dispersive effects on internal nonlinear waves in a sheared, stably stratified fluid layer". *Wave Motion*, in press, 1999.